

1 Full Title: **Uncoupling splicing from transcription using antisense oligonucleotides reveals**
2 **a dual role for I exon donor splice sites in antibody class switching**

3 Running title: **Antibody class switching modulation by antisense strategy**

4 Anne Marchalot^{a*}, Mohamad Omar Ashi^{a*}, Jean-Marie Lambert^a, Nivine Srour^a, Laurent
5 Delpy^{1,a\$} and Soazig Le Penne^{1,a\$}

6 ^a Unité Mixte de Recherche CNRS 7276 - INSERM 1262 - Université de Limoges, Limoges,
7 France.

8 ¹Corresponding authors: Soazig Le Penne^c (soazig.le-penne@unilim.fr) and Laurent Delpy
9 (laurent.delpy@unilim.fr), Université de Limoges - UMR CNRS 7276 - INSERM 1262, 2 rue
10 du Dr. Marcland, F-87025 Limoges, France, Fax # 33 555 435 897; Phone # 33 519 564 214.

11 * These authors contributed equally to the work, as co-first authors

12 \$ These authors contributed equally to the work, as co-last authors

13 This work was supported by grants from Fondation ARC (PJA 20161204724), INCa
14 (PLBIO15-256), ANR (2017-CE15-0024-01), Ligue Contre le Cancer (CD87, CD19, CD23),
15 and Fondation Française pour la Recherche contre le Myélome et les Gammopathies
16 monoclonales (FFRMG).

17

18 **ABSTRACT**

19 Class switch recombination (CSR) changes antibody isotype by replacing C μ constant exons
20 with different constant exons located downstream on the immunoglobulin heavy (*IgH*) locus.
21 During CSR, transcription through specific switch (S) regions and processing of noncoding
22 germline transcripts (GLTs) are essential for the targeting of Activation-Induced cytidine
23 Deaminase (AID). While CSR to IgG1 is abolished in mice lacking I γ 1 exon donor splice site
24 (dss), many questions remain regarding the importance of I exon dss recognition in CSR. To
25 further clarify the role of I exon dss in CSR, we first evaluated RNA polymerase II (RNA pol
26 II) loading and chromatin accessibility in S regions after activation of mouse B cells lacking
27 I γ 1 dss. We found that deletion of I γ 1 dss markedly reduced RNA pol II pausing and active
28 chromatin marks in the S γ 1 region. We then challenged the post-transcriptional function of I
29 exon dss in CSR by using antisense oligonucleotides (ASO) masking I exon dss on GLTs.
30 Treatment of stimulated B cells with an ASO targeting I γ 1 dss, in the acceptor S γ 1 region, or
31 I μ dss, in the donor S μ region, did not decrease germline transcription but strongly inhibited
32 constitutive splicing and CSR to IgG1. Altogether, this study reveals that the recognition of I
33 exon dss first supports RNA pol II pausing and the opening of chromatin in targeted S regions
34 and that GLTs splicing events using constitutive I exon dss appear mandatory for the later steps
35 of CSR, most likely by guiding AID to S regions.

36

37

38

39 INTRODUCTION

40 During immune responses, B cells can diversify the immunoglobulin (Ig) repertoire through
41 class switch recombination (CSR) and somatic hypermutation (SHM). SHM introduces
42 mutations in the variable (V) regions of Ig genes modifying antibody affinity for a cognate
43 antigen. The mouse Ig heavy chain (*IgH*) locus is comprised of eight constant genes (C_H). CSR
44 involves long-range interactions at the *IgH* locus and occurs between GC-rich repetitive switch
45 (S) DNA regions preceding each C_H gene due to the enzymatic activity of Activation-Induced
46 Deaminase (AID)^{1,2}. Thus, CSR replaces the C_μ exons by a downstream constant gene C_γ , C_ϵ
47 or C_α allowing expression of antibodies with different isotypes (from IgM to IgG, IgE or IgA)
48 and effector functions.

49 Transcription through S regions is required for CSR³. Germline (GL) transcription is initiated
50 from intervening (I) promoters a few kilobases upstream of both the donor and the acceptor S
51 regions. The μ I promoter drives constitutive transcription through S_μ while γ , ϵ or α I
52 promoters are inducible. Primary GL transcripts (GLTs) exhibit a conserved structure
53 composed of a noncoding I exon, an intronic S region and C_H exons^{4,5}. In mature GLTs, the I
54 exon is spliced to the first exon (CH1) of the adjacent constant gene. Because multiple stop
55 codons are present in the three reading frames of I exons, these GLTs do not encode peptides
56 of significant lengths.

57 During CSR, AID initiates double-strand DNA breaks (DSBs) by deaminating cytidines inside
58 the transcribed S regions. GL transcription through S regions of C_H gene favors AID
59 accessibility to S regions³. GL transcription promotes generation of RNA:DNA hybrid
60 structures (R-loops)^{6,7} revealing single-stranded DNA (ssDNA) that serves as substrate for AID
61⁸. The impairment of transcription elongation upon R-loop formation⁹ may favor RNA
62 polymerase II (RNA pol II) pausing. RNA pol II pausing then promotes AID recruitment to S
63 regions^{10,11}. Paused RNA pol II and histone modifications associated with “open” chromatin,

64 such as histone H3 lysine 4 trimethylation (H3K4me3) and histone H3 lysine 9 acetylation
65 (H3K9ac), are enriched in transcribed I-S regions and have been involved in AID targeting to
66 S regions primed for CSR¹²⁻¹⁶. Moreover, the Suppressor of Ty 5 homolog (Spt5) transcription
67 elongation factor and the RNA exosome, a cellular RNA-processing degradation complex,
68 associate with AID together with paused RNA pol II in transcribed S regions and are required
69 for CSR^{17,18}.

70 Beyond the prerequisite transcription of S regions, splicing of GLTs has been proposed to be
71 important for the CSR process. Notably, CSR to IgG1 is severely impaired in a mouse model
72 lacking the I γ 1 exon donor splice site (dss)^{19,20}. Further supporting a role for splicing of GLTs
73 in CSR, several RNA processing and splicing factors are critical regulators of CSR^{21,22}.

74 Interestingly, it has recently been proposed that intronic switch RNAs produced by the splicing
75 of primary GLTs act as guide RNAs and target AID to DNA in a sequence-specific manner²³.

76 After lariat debranching by the RNA debranching enzyme (DBR1), these switch RNAs are
77 folded into G-quadruplexes. G-quadruplexes and AID are targeted to S region DNA through
78 post-transcriptional action of the DEAD-box RNA helicase 1 (DDX1)²⁴.

79 Even though these data suggest that processing of GLTs by the splicing machinery is necessary
80 for CSR, the precise role of I exon dss recognition in antibody class switching remains largely
81 unknown. To address this issue, we first analysed whether the presence of I γ 1 exon dss could
82 influence RNA pol II pausing and chromatin accessibility of S γ 1 region, as early events leading
83 to CSR to IgG1. For that, Chromatin Immunoprecipitation (ChIP) experiments were performed
84 in stimulated B cells from the previously described human Metallothionein II_A (*hMT*) and *s-*
85 *hMT* (splice hMT) mouse models, lacking or harbouring I γ 1 exon dss, respectively^{19,20}. We
86 next specifically evaluated the impact of GLTs splicing on CSR to IgG1 by using antisense
87 oligonucleotides (ASOs) targeting specific I exon dss on primary GLTs, from both donor and
88 acceptor S regions. Contrary to the models used previously to study the impact of I exons on

89 CSR, treatment of mouse B cells by ASOs masks only a short RNA sequence (23 to 25
90 nucleotides) surrounding the I exon dss on primary GLTs. This antisense strategy bypassing
91 the impact of I exon dss recognition on transcription is very useful for studying the involvement
92 of I exon dss recognition in CSR at the post-transcriptional level. Collectively, our data indicate
93 that the recognition of I exon dss exerts both transcriptional and post-transcriptional roles
94 during CSR.

95

96 RESULTS

97 RNA pol II pausing and histone modifications upstream of the $S\gamma 1$ region are altered in 98 mice lacking $I\gamma 1$ dss

99 To clarify the role of I exon dss in CSR, we first performed comparative experiments in
100 homozygous *s-hMT* and *hMT* mice^{19,20}. In these models, the promoter and $I\gamma 1$ exon have been
101 replaced by the lipopolysaccharide (LPS)-inducible *hMT* promoter and an artificial I_{hMT} exon
102 containing (*s-hMT*) or lacking (*hMT*) $I\gamma 1$ dss (Figure 1A). As previously described by Lorenz
103 and collaborators²⁰, IgG1 class switching was almost abolished in *hMT* mice, whereas CSR to
104 other Ig isotypes remained unaffected (Supplementary figure 1A-C). This was not associated
105 with a difference in AID mRNA expression between splenic B cells isolated from *hMT* and *s-*
106 *hMT* mice (Supplementary figure 1D). Previous nuclear run-on assays have shown that the
107 transcription rate of the $S\gamma 1$ region was higher in LPS-stimulated B cells from *s-hMT* mice than
108 from *hMT* mice²⁰, suggesting a role for $I\gamma 1$ exon dss in GL transcription of the $S\gamma 1$ region. In
109 agreement with these results, we found low levels of unspliced $\gamma 1$ GLTs in LPS-stimulated B
110 cells from *hMT* mice, compared to *s-hMT* (Figure 1B).

111 Paused RNA pol II and histone modifications associated with “open” chromatin are involved
112 in AID recruitment to S regions during CSR^{10,12,13,15,16,18}. To study the role of I exon dss in
113 RNA pol II pausing and chromatin remodelling in the $S\gamma 1$ region, we performed ChIP
114 experiments in splenic B cells isolated from *hMT* and *s-hMT* mice after 2 days LPS stimulation.

115 First, antibodies directed against total RNA pol II, elongating RNA pol II (Ser2P) or pausing
116 RNA pol II (Ser5P) were used. In agreement with the low level of $\gamma 1$ GLTs described in Figure
117 1B, stimulated B cells from *hMT* mice displayed significantly decreased total RNA pol II
118 loading throughout the $S\gamma 1$ region, compared to *s-hMT* mice (Figure 1C). Interestingly, a
119 significant decrease in Ser5P RNA pol II loading (Figure 1D), but not Ser2P RNA pol II loading
120 (Figure 1E), was observed in the promoter- $S\gamma 1$ region in stimulated B cells from *hMT* compared
121 to *s-hMT* mice. Accordingly, stimulated B cells from *s-hMT* mice exhibited significantly higher
122 Ser5P/Ser2P ratios upstream from the $S\gamma 1$ region than B cells from *hMT* animals (Figure 1F),
123 suggesting that the recognition of I exon dss regulated RNA pol II pausing upstream from the
124 $S\gamma 1$ region. As a control, we found similar Ser5P and Ser2P RNA pol II loading in $S\mu$ and $S\gamma 2b$
125 regions in stimulated B cells from both *hMT* and *s-hMT* mice (Supplementary figure 2).

126 We next performed similar ChIP experiments using antibodies directed against variants of
127 histone H3. We observed very low levels of acetylated histone H3 (H3ac), a general marker of
128 chromatin accessibility, throughout the whole promoter- $S\gamma 1$ region in LPS-stimulated B cells
129 from *hMT* compared to *s-hMT* mice (Figure 1G). In addition, it has been previously shown that
130 H3K9ac and H3K4me3 levels in the region upstream from $S\gamma 1$ were very low in LPS-stimulated
131 B cells from *hMT* mice, compared to LPS + interleukin 4 (IL4)-stimulated B cells from wild
132 type (WT) mice²⁵. Therefore, to evaluate the specific enrichment of active histone marks in the
133 $S\gamma 1$ region in *hMT* and *s-hMT* models, H3K9ac and H3K4me3 levels were expressed as fold
134 change after normalisation to values obtained at the promoter. In B cells from *s-hMT* mice, the
135 highest levels of H3ac, H3K9ac and H3K4me3 histone forms were observed in the region
136 upstream from $S\gamma 1$ (Figure 1G-I). In contrast, this increase was not anymore observed in B cells
137 from *hMT* mice.

138 Collectively, our data indicate that I γ 1 exon dss recognition is of key importance for
139 transcriptional activity of the S γ 1 region by supporting RNA pol II pausing and chromatin
140 remodelling, two occurrences required for AID recruitment in S regions and efficient CSR.

141

142 **ASO strategy targeting I exon donor splice site allows uncoupling germline transcription** 143 **and splicing in wild type B cells**

144 We next wanted to study the function of I exon splicing on CSR. For this purpose, we treated
145 stimulated splenic B cells isolated from WT mice with vivo-morpholino antisense
146 oligonucleotide targeting the dss sequence of I γ 1 exon (I γ 1 dss ASO) (Figure 2A). Indeed, we
147 previously demonstrated that passive administration of these Phosphorodiamidate Morpholino
148 Oligonucleotides complexed with an octaguanidine dendrimer could very efficiently modulate
149 the splicing of Ig transcripts²⁶. First, we wanted to verify that masking the dss sequence of I γ 1
150 exon on GLTs by ASO did not inhibit γ 1 GL transcription. After 2 days culture with LPS + IL4
151 and 2 μ M ASO, expression of unspliced γ 1 GLTs in activated B cells was significantly
152 increased after treatment with I γ 1 dss ASO (Figure 2B), compared to cells treated with an
153 irrelevant control ASO. This suggested an accumulation of unspliced γ 1 GLTs due to I γ 1 dss
154 ASO-induced splicing inhibition. In order to study the consequences of I γ 1 dss ASO on spliced
155 γ 1 GLTs, we next performed PCR using the I γ 1-C γ 1 primer pair (I γ 1-for and C γ 1-rev, described
156 in Figure 2C and Supplementary table 1) on cDNA from ASO-treated WT splenic B cells
157 stimulated by LPS + IL4. After 2 days, the γ 1 GLTs profile was strikingly different in control
158 and I γ 1 dss ASO conditions (Figure 2C-up). A band corresponding to the constitutively spliced
159 γ 1 GLT (involving the constitutive I γ 1 exon dss) was strongly detected in control but slightly
160 detected upon I γ 1 dss ASO treatment (Figure 2C-up and Supplementary figure 3). Remarkably,
161 in both control and I γ 1 dss ASO conditions, additional bands were also detected that could
162 account for new splicing isoforms. Sanger sequencing indeed revealed alternative transcripts

163 so far not described in the literature (alternative transcripts 1, 2 and 3; Figure 2C-middle and
164 Supplementary figure 3) involving donor and acceptor splice sites internal to the I γ 1 exon. The
165 fact that these alternative splice sites were predicted with high consensus value by the HSF 3.1
166 tool (HSF 3.1, 24/07/2019, <http://www.umd.be/HSF/HSF.shtml>, ²⁷) (Figure 2C-down)
167 indicated that the different PCR products were *bona fide* spliced transcripts. As a proof of ASO
168 efficiency, treatment with I γ 1 dss ASO almost abolished the major constitutive GLT and
169 prevented alternative transcript 1 detection (Figure 2C-up). Thus, after treatment with I γ 1 dss
170 ASO, transcript isoforms using the constitutive I γ 1 dss represented only 20% of the detected
171 transcripts (*versus* 90% in control). Another consequence of I γ 1 dss ASO treatment is the
172 detection of alternative transcript 3 and a better detection of alternative transcript 2.
173 Since our data showed that I γ 1 dss ASO strongly decreased γ 1 GLT constitutive splicing, ASO
174 strategy is a good tool to study the function of I γ 1 exon splicing on CSR.

175

176 **Treatment with I γ 1 exon dss ASO specifically inhibits IgG1 class switching**

177 We next investigated the effect of ASO-mediated γ 1 GLTs splicing inhibition on CSR to IgG1.
178 After 3 days culture with LPS + IL4 and 2 μ M ASO, CSR to IgG1 was greatly diminished in B
179 cells treated with I γ 1 dss ASO compared to B cells treated with an irrelevant control ASO. The
180 percentage of IgG1 positive B cells determined by flow cytometry was decreased 4-fold in I γ 1
181 dss ASO-treated B cells (Figure 2D-E) and IgG1 levels determined in culture supernatants by
182 Enzyme Linked Immuno Sorbent Assay (ELISA) were almost 2-fold lower in I γ 1 dss ASO-
183 treated cells (Figure 2F) than in control B cells. In agreement with the CSR defect, I μ -C γ 1
184 switched transcripts were decreased by 4 fold in I γ 1 dss ASO-treated B cells (Figure 2G).
185 In order to control I γ 1 dss ASO specificity, we realized similar experiments in B cells stimulated
186 by anti-CD40 + IL4. Similarly to what observed in LPS + IL4 -stimulated B cells, after 2 days
187 culture with anti-CD40 + IL4 and 2 μ M ASO, expression of unspliced γ 1 GLTs was

188 significantly increased (Figure 3B) and CSR to IgG1 was significantly diminished (Figure 3C-
189 D) in B cells treated with I γ 1 dss ASO compared to B cells treated with an irrelevant control
190 ASO. However, expression of unspliced I ϵ GLTs (Figure 3E) and CSR to IgE (Figure 3F-G)
191 were similar in B cells treated with the irrelevant control ASO or I γ 1 dss ASO. This showed
192 that I γ 1 dss ASO specifically decreased CSR to IgG1 by inhibiting splicing precisely on γ 1
193 GLTs.

194 Collectively, these data indicate that splicing of γ 1 GLTs is necessary for CSR to IgG1 and
195 strongly suggest that the use of the constitutive I γ 1 exon dss during splicing is required for
196 efficient CSR.

197

198 **Treatment with an ASO targeting the constitutive I exon dss in the donor S μ region also**
199 **inhibits IgG1 class switching**

200 Our results showed that ASO strategy targeting the constitutive I exon dss from S γ 1 acceptor
201 region inhibited CSR to IgG1. We next developed a similar approach to determine whether
202 specifically masking the constitutive I exon dss from the donor S μ region could also inhibited
203 CSR to IgG1. Splenic B cells isolated from WT mice were stimulated by LPS + IL4 and treated
204 with an ASO targeting the constitutive I μ exon dss (I μ dss ASO) (Figure 4A). In order to study
205 the consequences of I μ dss ASO on spliced I μ GLTs, we performed PCR using the I μ -C μ primer
206 pair (I μ -for and C μ -rev, described in Figure 4A and Supplementary table 1) on cDNA from
207 stimulated splenic B cells treated with 2 μ M ASO for 2 days. A band corresponding to the
208 constitutively spliced I μ transcript (involving the constitutive I μ exon dss) was detected in
209 control but slightly detected after I μ dss ASO treatment (Figure 4B). Similarly to what observed
210 in stimulated splenic B cells treated with I γ 1 dss ASO, we detected the presence of alternatively
211 spliced I μ transcripts in cells treated with I μ dss ASO. These alternative transcripts were
212 indicative of the use of alternative I μ dss present in the intronic S region previously described

213 by Kuzin and collaborators²⁸. In addition, after 3 days culture with LPS + IL4 and 2 μ M ASO,
214 CSR to IgG1 was significantly diminished in B cells treated with I μ dss ASO compared to B
215 cells treated with an irrelevant control ASO (Figure 4C-D). After 2 days 2 μ M ASO treatment,
216 expression of unspliced γ 1 GLTs was similar in B cells treated with an irrelevant control or I μ
217 dss ASO (Figure 4E). This showed that the defect in IgG1 class switching observed after
218 treatment by I μ dss ASO was not due to an inhibition of γ 1 GLTs splicing but to the splicing
219 decrease of I μ GLTs.

220 Our results indicated that splicing of GLTs involving the constitutive I μ dss is necessary for
221 efficient CSR to IgG1. Therefore, correct splicing of GLTs produced in both the donor S μ and
222 the acceptor S γ 1 regions is required for efficient IgG1 class switching.

223
224
225

DISCUSSION

226 S region transcription *per se* promotes basal class switch recombination but, for optimal
227 efficiency, the process requires the presence of the intact I region, implicating factors beyond
228 transcription through the S region in the regulation of class switching²⁹. Transcription and pre-
229 mRNA processing are functionally coupled. In our study, through the experimental uncoupling
230 of splicing from transcription, we identified distinct functions of I exon dss that control antibody
231 class switching at transcriptional and post-transcriptional levels. During transcription, we
232 provide evidence that deletion of the I γ 1 exon dss decreased accumulation of Ser5P RNA pol
233 II and chromatin accessibility in the promoter-S γ 1 region. Moreover, our data demonstrated
234 that, in S regions primed for CSR, GLTs splicing involving the constitutive I exon dss is an
235 essential step for efficient CSR.

236 Regarding the impact of I exon dss on transcription, our comparative analysis of *s-hMT* and
237 *hMT* B cells indicated that, in the absence of I γ 1 dss, GL transcription and RNA pol II loading
238 were very weak at the γ 1 locus. Interestingly, RNA pol II binding was strongly diminished at
239 the *hMT* promoter, suggesting that the presence of I γ 1 exon dss enhanced the initiation of GL

240 transcription. These data are consistent with the poor transcription observed upon deletion of a
241 large portion of I γ 2b exon including dss³⁰. Although the function of I exon dss in transcription
242 regulation has been overlooked, such intron-mediated enhancement of gene expression has long
243 been described in a wide range of organisms, including mammals³¹. Indeed, it has been
244 demonstrated that the presence of a dss facilitates the transcription preinitiation complex
245 assembly and stimulates transcription even in the absence of splicing^{32,33}. Whether the
246 recognition of I exon dss promotes the formation of pre-initiation complex³² and involves a
247 gene looping interaction between promoter and dss, as described in yeast cells³⁴, remains to be
248 investigated. Our ChIP analysis further indicated that, in the absence of I γ 1 exon dss, RNA pol
249 II pausing is markedly decreased in the promoter-S γ 1 region, whereas the rate of RNA pol II
250 elongation remains mostly unchanged. It is tempting to speculate that the I exon dss acts as an
251 anchor for the co-transcriptional machinery and is required for appropriate associations of
252 critical factors, like Spt5, with RNA pol II to enable recruitment of AID to S regions. After B
253 cells stimulation, transcribed I-S regions are a focus for increased modified histones, such as
254 H3ac, H3K9ac or H3K4me3, and chromatin accessibility^{13,16}. Reinforcing the idea that GL
255 transcription, RNA pol II pausing and the establishment of active chromatin marks in S regions
256 are interconnected¹⁰, we found a global reduction of active H3ac marks in the promoter-S γ 1
257 region of stimulated B cells from *hMT* mice, compared to *s-hMT*. The H3K9ac and H3K4me3
258 enrichment specifically detected upstream the S γ 1 region was also lost in *hMT* mice.
259 Interestingly, it has been proposed that H3K4me3 serves as a mark for recruiting the
260 recombinase machinery for CSR independently of its function in transcription^{15,35}. These
261 studies have shown that Spt5 and the histone chaperone FAcilitates Chromatin Transcription
262 (FACT) are not required for transcription of S regions but regulate H3K4me3 modification and
263 DNA cleavage in CSR^{15,35}.

264 I γ 1 exon dss recognition is necessary for the regulation of GL transcription. Consequently,
265 using classical I exon deletion and/or replacement mouse models neither allow distinguishing
266 the roles of I exon dss in the interconnected processes of transcription and splicing nor permit
267 distinguishing between requirements of splicing *per se* from that of stable S GLTs³⁶. Several
268 studies including ours have shown the efficacy of ASO-mediated approaches to modify RNA
269 splicing in B-lineage cells^{26,37,38}. Here, we used ASOs targeting short sequence (23 to 25
270 nucleotides) spanning the I γ 1 or I μ exon dss on pre-mRNA to analyse the consequences of
271 GLTs splicing defect on CSR to IgG1 in splenic B cells from WT mice. We showed that, in
272 addition to its positive effect on transcription, I exon dss recognition is required at the post-
273 transcriptional level for efficient CSR to IgG1. Moreover, our results strongly suggest that
274 splicing of GLTs *per se* is not sufficient to induce CSR. Indeed, we found a marked reduction
275 of CSR to IgG1 upon treatment with ASOs masking constitutive I exon dss on GLTs produced
276 in the donor S μ or the acceptor S γ 1 regions, even though alternative splicing events could be
277 readily detected. By contrast, Kuzin and collaborators showed normal surface Ig expression and
278 serum Ig levels in Δ I μ -s^{-/-} mice harbouring a deletion of 236 bp spanning the constitutive I μ dss
279²⁸. As expected, there were no detectable spliced I μ transcripts in these mice. Nevertheless,
280 alternative “I μ -like” GLTs driven by regulatory elements other than E μ were detected at low
281 levels in B cells from Δ I μ -s^{-/-} mice. The authors suggested that such alternative “I μ -like” GLTs
282 directly contribute to CSR activity²⁸. However, our results showed that these alternative “I μ -
283 like” GLTs might not be sufficient for efficient CSR activity *in vitro*. Indeed, after treatment of
284 B cells with I μ dss ASO, we detected I μ -C μ alternative transcripts indicative of the use of the
285 same cryptic S μ dss than described by Kuzin and collaborators whereas a drastic inhibition of
286 CSR was observed. The regulation of μ locus is complex and further investigations are needed
287 to understand the discrepancies concerning the impact of I μ dss absence at the DNA level, in
288 genetically modified mouse model, and at the RNA level, with our ASO strategy, on CSR.

289 Nonetheless, our data are in agreement with a study of Ruminy and collaborators ³⁹. They
290 detected recurrent acquired mutations at the I μ dss on the functional *IgH* allele of t(14;18)
291 positive lymphomas cases presenting restricted IgM expression and proposed that disruption of
292 I μ constitutive dss, inducing the expression of abnormal GLTs, may be involved in the
293 perturbation of CSR observed in these lymphomas. Moreover, Spt4 depletion by siRNA in the
294 CH12F3-2A B cell line severely impaired CSR to IgA despite a dramatically increased
295 expression of cryptic transcripts initiating from the S μ intronic region ³⁵. As observed in the
296 donor S μ region, masking the constitutive I exon dss on GLTs produced in the acceptor S γ 1
297 region with I γ 1 dss ASO strongly inhibited CSR to IgG1 despite I γ 1-C γ 1 alternative transcripts
298 were detectable. Additional molecular studies will be required to delineate the mechanism
299 involved in the ASO-mediated inhibition of CSR. Several scenarios could explain the inhibition
300 of CSR to IgG1 by I exon dss ASOs. First, RNA-binding proteins have been shown to interact
301 with AID ^{22,40-42} and the ASO, attached to the GLTs, could avoid fixation of such proteins
302 necessary for CSR. Second, it has been described that, when the accumulation of intronic switch
303 RNAs was prevented from the onset of CH12F3-2A B cells stimulation, R-loop levels were
304 decreased by half in S regions ²⁴. In our study, after I exon dss ASO treatment, the accumulation
305 of unspliced GLTs indicated a strong splicing inhibition. Thus, even though low levels of
306 constitutive and alternative spliced GLTs are detected after ASO treatment, the lariat abundance
307 may be too weak to induce R-loop formation at S regions and efficient CSR. Third, even if
308 alternatively spliced GLTs were detected after ASOs treatments, the sequence of intronic lariat
309 generated after alternative splicing could prevent efficient CSR. For example, alternative lariat
310 sequence could impede the lariat debranching by DBR1 and the subsequent generation of G-
311 quadruplex RNA structures that participate in guiding AID to specific S regions through
312 RNA:DNA base-pairing ²³. Alternative lariat sequence could also avoid the fixation of DDX1
313 to G-quadruplex switch RNAs and consequently impair AID binding to S regions DNA ²⁴.

314 These explanations are consistent with a model whereby processed S region transcripts serve
315 as guide RNAs to target AID, in a sequence-dependent manner, to the S regions DNA from
316 which they were transcribed³⁶.

317 In summary, our study highlighted a dual role for I exon dss during CSR, at the DNA and RNA
318 levels, and further paves the way for antisense strategies in the modulation of antibody class
319 switching and immune response efficiency.

320

321 **MATERIALS AND METHODS**

322 **Mice**

323 Two to six month-old *C57BL/6*, *s-hMT* and *hMT* mice were used. *hMT* and *s-hMT* mice were
324 kindly obtained from Dr. A. Radbruch (Leibniz Institute, Berlin, Germany). Mice were housed
325 and procedures were conducted in agreement with european directive 2010/63/EU on animals
326 used for scientific purposes applied in France as the 'Décret n°2012-118 du 1er février 2013
327 relatif à la protection des animaux utilisés à des fins scientifiques'. Accordingly, the present
328 project APAFIS#15279-2018052915087229 v3 was authorized by the 'Ministère de l'Education
329 Nationale, de l'Enseignement Supérieur et de la Recherche'.

330

331 **Splenic B cell *in vitro* stimulation and ASO treatments**

332 Splenic B cells isolated from *C57BL/6*, *hMT* and *s-hMT* mice were purified with the EasySep
333 Mouse B Cell Isolation Kit (Stemcell Technologies). B cells were cultured for 2 to 4 days in
334 RPMI 1640 with UltraGlutamine (Lonza) containing 10% fetal calf serum (FCS) (Dominique
335 Dutscher), 1 mM sodium pyruvate (Eurobio), 1% AANE (Eurobio), 50 U/ml penicillin / 50
336 µg/ml streptomycin (Gibco) and 129 µM 2-mercaptoethanol (Sigma-Aldrich). Splenic B cells
337 were stimulated with either 1 µg/ml LPS (LPS-EB Ultrapure, InvivoGen), 1 µg/ml LPS + 20
338 ng/ml IL4 (Recombinant Murine IL-4, PeproTech) or 5 µg/ml anti-CD40 (mouse
339 CD40/TNFRSF5 MAb (Clone 1C10), Biotechne, USA) + 40 ng/ml IL4. For ASO treatments,

340 vivo-morpholino ASOs (*I γ 1* dss ASO: 5'-CCCACTCCCCTGGTCACTTACCG-3'; *I μ* dss
341 ASO: 5'-GGCTGCCTCTGGCTTACCATTG-3') and an irrelevant ASO (control: 5'-
342 CCTCTTACCTCAGTTACAATTTATA-3') were designed and purchased at Gene Tools, LLC
343 (Philomath, USA). Stimulated splenic B cells were cultured in the presence of 2 μ M ASO.
344 Culture samples were harvested at day 2, 3 or 4 for subsequent flow cytometry analysis, ChIP
345 assays or RNA extraction. Supernatants of stimulated B cells were collected at day 3 or 4 and
346 stored at -20°C until used for ELISA assays.

347

348 **Flow cytometry**

349 Cell suspensions of *in vitro* stimulated splenic B cells were washed in phosphate-buffered saline
350 (PBS). To reduce Fc receptor-mediated binding by antibodies of interest, B cells were pre-
351 incubated during 15 minutes with 0.5 μ g/ml anti-mouse CD16/CD32 (Clone 2.4G2, BD
352 Pharmingen, ref 553142) in FACS buffer (PBS supplemented with 2% FCS and 2 mM
353 (Ethylenedinitrilo)tetraacetic acid (EDTA) (Sigma-Aldrich)). Cells were then labelled with 0.5
354 μ g/ml anti-mouse B220-BV421 (clone RA3-6B2, BioLegend, ref 103240) and 0.5 μ g/ml anti-
355 mouse IgG1-FITC (clone A85-1, BD Pharmingen, ref 553443) antibodies. After 45 minutes,
356 cells were washed in PBS and suspended in FACS buffer. For non-viable cells exclusion, 5 μ l
357 of 7-AAD (BD Pharmingen, ref 559925) were added on cells 10 minutes before flow cytometry
358 analysis. Data were acquired on a BD Pharmingen Fortessa LSR2 (BD Biosciences, San Jose,
359 CA, USA) and analysed using Flowlogic™ software (Miltenyi Biotec).

360

361 **ELISA assays**

362 Culture supernatants and sera were analysed for the presence of IgM, IgG1 or IgG2b by ELISA.
363 Blood samples were collected from 12 weeks-old *hMT* and *s-hMT* mice. Serum samples were
364 recovered by centrifugation and stored at -20°C until used. ELISA assays were performed in
365 polycarbonate 96 multiwell plates, coated overnight at 4°C (100 μ l per well) with 2 μ g/ml IgM,

366 IgG1 or IgG2b antibodies (Southern Biotechnologies: goat anti-Mouse IgM human ads UNLB,
367 ref 1020-01; goat anti-Mouse IgG1 Human ads-UNLB, ref 1070-01; goat anti-Mouse IgG2b
368 Human ads-UNLB, ref 1090-01) in PBS. After three successive washing steps in PBS with
369 0.05% Tween® 20 (Sigma-Aldrich), a blocking step with 100 µl of 3% bovine serum albumin
370 (BSA) (Euromedex) in PBS was performed for 30 min at 37°C. After three washing steps, 50
371 µl of sera / supernatant, or standards IgM, IgG1 or IgG2b (Southern Biotechnologies, 400
372 ng/ml) were diluted into successive wells in 1% BSA/PBS buffer and incubated for 2 h at 37°C.
373 After three washing steps, 100 µl per well of 1 µg/ml Alkaline Phosphatase (AP)-conjugated
374 goat anti-mouse antibodies (Southern Biotechnologies: goat anti-Mouse IgG1 Human ads-AP,
375 ref 1070-04 and goat anti-mouse kappa-AP, ref 1050-04 ; Cell Lab: goat anti-Mouse IgG2b
376 Human ads-AP, ref 731943) were incubated in PBS with 0.05% Tween® 20 for 2 h at 37°C.
377 After three washing steps, AP activity was assayed: 100 µl of substrate for AP (SIGMAFAST™
378 p-Nitrophenyl phosphate Tablets, Sigma-Aldrich) were added and, after 15 min, the reaction
379 was blocked with addition of 50 µl of 3 M NaOH (Sigma-Aldrich). Optic density was then
380 measured at 405 nm on a Multiskan FC microplate photometer (Thermo Scientific).

381

382 **RT-PCR and quantitative RT-PCR**

383 *In vitro* stimulated splenic B cells were harvested and RNA was extracted using TRIzol™
384 Reagent (Invitrogen) procedure. Reverse transcription was carried out on 1 µg of DNase I
385 (Invitrogen)-treated RNA using High-Capacity cDNA Reverse Transcription kit (Applied
386 Biosystems). Priming for reverse transcription was done with random hexamers.

387 To analyse GL transcription, PCRs were performed on cDNA using the Taq Core Kit (MP
388 Biomedicals) and appropriate primer pairs (primer pairs are provided in Supplementary table
389 1). PCR amplification of the β-actin transcript was used as an internal loading control.

390 To determine nucleotide sequence of normal and alternative transcripts, PCRs were performed
391 on cDNA using the Phusion[®] High-Fidelity DNA Polymerase (New England BioLabs) and
392 appropriate primer pairs. After purification of the RT-PCR products using the NucleoSpin Gel
393 and PCR Clean-up kit (Macherey-Nagel) according to the manufacturer's instructions,
394 sequencing was performed using the BigDye[™] Terminator v3.1 Cycle Sequencing Kit on a
395 3130xl Genetic Analyzer ABI PRISM (Applied Biosystems). Quantification of the purified RT-
396 PCR products was also performed using an Agilent 2100 Bioanalyzer (Agilent Technologies)
397 according to the Agilent High Sensitivity DNA kit instructions.

398 Quantitative PCRs were performed on cDNA using Premix Ex Taq[™] (probe qPCR), ROX Plus
399 (Takara) or TB Green Premix Ex Taq[™] II (Tli RNase H Plus), ROX Plus (Takara) on a
400 StepOnePlus Real-Time PCR system (Applied Biosystems). Transcripts were quantified
401 according to the standard $2^{-\Delta\Delta Ct}$ method after normalization to *Gapdh*. Primers and probes used
402 for determination of transcripts are listed in Supplementary table 1.

403

404 **ChIP assays**

405 ChIP assays were performed using anti-H3ac (Millipore, 06-599), anti-H3K4me3 (Millipore,
406 07-473), anti-H3K9ac (Millipore, 06-942), anti-RNA pol II (CTD4H8, Santa Cruz
407 Biotechnology, sc-47701), anti-RNA pol II ser2P (Abcam, ab5095), and anti-RNA pol II ser5P
408 (Abcam, ab5131) as previously described⁴³. In brief, 1×10^7 LPS stimulated B cells from *hMT*
409 and *s-hMT* mice were harvested at day 2, washed twice in PBS and cross-linked at 37°C for 15
410 min in 15 ml of PBS with 1% formaldehyde (Sigma-Aldrich). The reaction was quenched with
411 0.125 M glycine (Sigma-Aldrich). After lysis, chromatin was sonicated to 0.5–1 kb using a
412 Vibracell 75043 (Thermo Fisher Scientific). After dilution in ChIP buffer (0.01% SDS (Sigma-
413 Aldrich), 1.1% Triton X-100 (Sigma-Aldrich), 1.2 mM EDTA (Eurobio), 16.7mM Tris-HCl
414 (Sigma-Aldrich), pH 8.1, and 167 mM NaCl (Sigma-Aldrich)), chromatin was precleared by

415 rotating for 2 h at 4°C with 100 µl of 50% protein A/G slurry (0.2 mg/ml sheared salmon sperm
416 DNA, 0.5 mg/ml BSA, and 50% protein A/G; Sigma-Aldrich), 0.3–0.5×10⁶ cell equivalents
417 were saved as input, and 3–5×10⁶ cell equivalents were incubated overnight with specific or
418 control antibodies. Immune complexes were precipitated by the addition of protein A/G. Cross-
419 linking was reversed by overnight incubation (70°C) in Tris-EDTA (Sigma-Aldrich) buffer
420 with 0.02% SDS, and genomic DNA was obtained after phenol/chloroform extraction. Analysis
421 of immuno-precipitated DNA sequences was done by quantitative PCR using the primer pairs
422 described in Supplementary table 1.

423

424 **Statistical analysis**

425 Results are expressed as means ± SEM and overall differences between variables were
426 evaluated by an unpaired two-tailed Student's *t* test using Prism GraphPad software (San Diego,
427 CA).

428

429 **ACKNOWLEDGEMENTS**

430 We thank the staff of our animal facility. We also thank J. Cook-Moreau and E. Pinaud (UMR
431 CNRS 7276 – INSERM 1262, Limoges, France) for critical reading of the manuscript and A.
432 Radbruch (Leibniz Institute, Berlin, Germany) for providing *hMT* and *s-hMT* mice. This work
433 was supported by grants from Fondation ARC (PJA 20161204724), INCa (PLBIO15-256),
434 ANR (2017-CE15-0024-01), Ligue Contre le Cancer (CD87, CD19, CD23), and Fondation
435 Française pour la Recherche contre le Myélome et les Gammopathies monoclonales (FFRMG).

436

437 **AUTHOR CONTRIBUTIONS**

438 AM and MOA performed experiments and analysed data. JML and NS performed experiments.
439 SLP and LD conceived the project, designed experiments, analysed data and wrote the
440 manuscript.

441

442 SUPPLEMENTARY MATERIAL

443 The online version of this article contains supplementary material.

444

445 CONFLICT OF INTEREST

446 The authors declare no conflict of interest.

447

448 REFERENCES

- 449 1 Arakawa H. Requirement of the Activation-Induced Deaminase (AID) Gene for
450 Immunoglobulin Gene Conversion. *Science* 2002; **295**: 1301–1306.
- 451 2 Muramatsu M, Kinoshita K, Fagarasan S, Yamada S, Shinkai Y, Honjo T. Class Switch
452 Recombination and Hypermutation Require Activation-Induced Cytidine Deaminase
453 (AID), a Potential RNA Editing Enzyme. *Cell* 2000; **102**: 553–563.
- 454 3 Matthews AJ, Zheng S, DiMenna LJ, Chaudhuri J. Regulation of Immunoglobulin Class-
455 Switch Recombination. In: *Advances in Immunology*. Elsevier, 2014, pp 1–57.
- 456 4 Lennon GG, Perry RP. C mu-containing transcripts initiate heterogeneously within the IgH
457 enhancer region and contain a novel 5'-nontranslatable exon. *Nature* 1985; **318**: 475–478.
- 458 5 Lutzker S, Alt FW. Structure and expression of germ line immunoglobulin gamma 2b
459 transcripts. *Mol Cell Biol* 1988; **8**: 1849–1852.
- 460 6 Tian M, Alt FW. Transcription-induced Cleavage of Immunoglobulin Switch Regions by
461 Nucleotide Excision Repair Nucleases *in Vitro*. *Journal of Biological Chemistry* 2000; **275**:
462 24163–24172.
- 463 7 Yu K, Chedin F, Hsieh C-L, Wilson TE, Lieber MR. R-loops at immunoglobulin class
464 switch regions in the chromosomes of stimulated B cells. *Nature Immunology* 2003; **4**: 442–
465 451.
- 466 8 Chaudhuri J, Tian M, Khuong C, Chua K, Pinaud E, Alt FW. Transcription-targeted DNA
467 deamination by the AID antibody diversification enzyme. *Nature* 2003; **422**: 726–730.
- 468 9 Huertas P, Aguilera A. Cotranscriptionally Formed DNA:RNA Hybrids Mediate
469 Transcription Elongation Impairment and Transcription-Associated Recombination.
470 *Molecular Cell* 2003; **12**: 711–721.
- 471 10 Kenter AL. AID targeting is dependent on RNA polymerase II pausing. *Seminars in*
472 *Immunology* 2012; **24**: 281–286.
- 473 11 Pavri R, Nussenzweig MC. AID Targeting in Antibody Diversity. In: *Advances in*
474 *Immunology*. Elsevier, 2011, pp 1–26.

- 475 12 Daniel JA, Nussenzweig A. The AID-Induced DNA Damage Response in Chromatin.
476 *Molecular Cell* 2013; **50**: 309–321.
- 477 13 Jeevan-Raj BP, Robert I, Heyer V, Page A, Wang JH, Cammas F *et al.* Epigenetic tethering
478 of AID to the donor switch region during immunoglobulin class switch recombination. *The*
479 *Journal of Experimental Medicine* 2011; **208**: 1649–1660.
- 480 14 Kuang FL, Luo Z, Scharff MD. H3 trimethyl K9 and H3 acetyl K9 chromatin modifications
481 are associated with class switch recombination. *Proceedings of the National Academy of*
482 *Sciences* 2009; **106**: 5288–5293.
- 483 15 Stanlie A, Aida M, Muramatsu M, Honjo T, Begum NA. Histone3 lysine4 trimethylation
484 regulated by the facilitates chromatin transcription complex is critical for DNA cleavage in
485 class switch recombination. *Proceedings of the National Academy of Sciences* 2010; **107**:
486 22190–22195.
- 487 16 Wang L, Wuerffel R, Feldman S, Khamlichi AA, Kenter AL. S region sequence, RNA
488 polymerase II, and histone modifications create chromatin accessibility during class switch
489 recombination. *The Journal of Experimental Medicine* 2009; **206**: 1817–1830.
- 490 17 Basu U, Meng F-L, Keim C, Grinstein V, Pefanis E, Eccleston J *et al.* The RNA Exosome
491 Targets the AID Cytidine Deaminase to Both Strands of Transcribed Duplex DNA
492 Substrates. *Cell* 2011; **144**: 353–363.
- 493 18 Pavri R, Gazumyan A, Jankovic M, Di Virgilio M, Klein I, Ansarah-Sobrinho C *et al.*
494 Activation-Induced Cytidine Deaminase Targets DNA at Sites of RNA Polymerase II
495 Stalling by Interaction with Spt5. *Cell* 2010; **143**: 122–133.
- 496 19 Hein K, Lorenz MGO, Siebenkotten G, Petry K, Christine R, Radbruch A. Processing of
497 Switch Transcripts Is Required for Targeting of Antibody Class Switch Recombination.
498 *The Journal of Experimental Medicine* 1998; **188**: 2369–2374.
- 499 20 Lorenz M, Jung S, Radbruch A. Switch transcripts in immunoglobulin class switching.
500 *Science* 1995; **267**: 1825–1828.
- 501 21 Conticello SG, Ganesh K, Xue K, Lu M, Rada C, Neuberger MS. Interaction between
502 Antibody-Diversification Enzyme AID and Spliceosome-Associated Factor CTNNB1.
503 *Molecular Cell* 2008; **31**: 474–484.
- 504 22 Nowak U, Matthews AJ, Zheng S, Chaudhuri J. The splicing regulator PTBP2 interacts
505 with the cytidine deaminase AID and promotes binding of AID to switch-region DNA.
506 *Nature Immunology* 2011; **12**: 160–166.
- 507 23 Zheng S, Vuong BQ, Vaidyanathan B, Lin J-Y, Huang F-T, Chaudhuri J. Non-coding RNA
508 Generated following Lariat Debranching Mediates Targeting of AID to DNA. *Cell* 2015;
509 **161**: 762–773.
- 510 24 Ribeiro de Almeida C, Dhir S, Dhir A, Moghaddam AE, Sattentau Q, Meinhart A *et al.*
511 RNA Helicase DDX1 Converts RNA G-Quadruplex Structures into R-Loops to Promote
512 IgH Class Switch Recombination. *Molecular Cell* 2018; **70**: 650–662.e8.

- 513 25 Feldman S, Achour I, Wuerffel R, Kumar S, Gerasimova T, Sen R *et al.* Constraints
514 Contributed by Chromatin Looping Limit Recombination Targeting during Ig Class Switch
515 Recombination. *Jl* 2015; **194**: 2380–2389.
- 516 26 Ashi MO, Srour N, Lambert J-M, Marchalot A, Martin O, Le Noir S *et al.* Physiological
517 and druggable skipping of immunoglobulin variable exons in plasma cells. *Cellular &*
518 *Molecular Immunology* 2019; **16**: 810–819.
- 519 27 Desmet F-O, Hamroun D, Lalande M, Collod-Bérout G, Claustres M, Bérout C. Human
520 Splicing Finder: an online bioinformatics tool to predict splicing signals. *Nucleic Acids*
521 *Research* 2009; **37**: e67–e67.
- 522 28 Kuzin II, Ugine GD, Wu D, Young F, Chen J, Bottaro A. Normal Isotype Switching in B
523 Cells Lacking the I μ Exon Splice Donor Site: Evidence for Multiple I μ -Like Germline
524 Transcripts. *The Journal of Immunology* 2000; **164**: 1451–1457.
- 525 29 Bottaro A, Lansford R, Xu L, Zhang J, Rothman P, Alt FW. S region transcription per se
526 promotes basal IgE class switch recombination but additional factors regulate the efficiency
527 of the process. *The EMBO Journal* 1994; **13**: 665–674.
- 528 30 Seidl KJ, Bottaro A, Vo A, Zhang J, Davidson L, Alt FW. An expressed neo(r) cassette
529 provides required functions of the I γ 2b exon for class switching. *Int Immunol* 1998;
530 **10**: 1683–1692.
- 531 31 Shaul O. How introns enhance gene expression. *The International Journal of Biochemistry*
532 *& Cell Biology* 2017; **91**: 145–155.
- 533 32 Damgaard CK, Kahns S, Lykke-Andersen S, Nielsen AL, Jensen TH, Kjems J. A 5' Splice
534 Site Enhances the Recruitment of Basal Transcription Initiation Factors In Vivo. *Molecular*
535 *Cell* 2008; **29**: 271–278.
- 536 33 Furger A. Promoter proximal splice sites enhance transcription. *Genes & Development*
537 2002; **16**: 2792–2799.
- 538 34 Moabbi AM, Agarwal N, El Kaderi B, Ansari A. Role for gene looping in intron-mediated
539 enhancement of transcription. *Proceedings of the National Academy of Sciences* 2012; **109**:
540 8505–8510.
- 541 35 Stanlie A, Begum NA, Akiyama H, Honjo T. The DSIF Subunits Spt4 and Spt5 Have
542 Distinct Roles at Various Phases of Immunoglobulin Class Switch Recombination. *PLoS*
543 *Genetics* 2012; **8**: e1002675.
- 544 36 Yewdell WT, Chaudhuri J. A transcriptional serenAID: the role of noncoding RNAs in
545 class switch recombination. *International Immunology* 2017; **29**: 183–196.
- 546 37 Bestas B, Moreno PMD, Blomberg KEM, Mohammad DK, Saleh AF, Sutlu T *et al.* Splice-
547 correcting oligonucleotides restore BTK function in X-linked agammaglobulinemia model.
548 *Journal of Clinical Investigation* 2014; **124**: 4067–4081.
- 549 38 Dewaele M, Tabaglio T, Willekens K, Bezzi M, Teo SX, Low DHP *et al.* Antisense
550 oligonucleotide-mediated MDM4 exon 6 skipping impairs tumor growth. *Journal of*
551 *Clinical Investigation* 2015; **126**: 68–84.

- 552 39 Ruminy P, Jardin F, Penther D, Picquenot J-M, Parmentier F, Buchonnet G *et al.* Recurrent
553 disruption of the I μ splice donor site in t(14;18) positive lymphomas : A potential molecular
554 basis for aberrant downstream class switch recombination. *Genes, Chromosomes and*
555 *Cancer* 2007; **46**: 735–744.
- 556 40 Chen J, Cai Z, Bai M, Yu X, Zhang C, Cao C *et al.* The RNA-binding protein ROD1/PTBP3
557 cotranscriptionally defines AID-loading sites to mediate antibody class switch in
558 mammalian genomes. *Cell Research* 2018; **28**: 981–995.
- 559 41 Hu W, Begum NA, Mondal S, Stanlie A, Honjo T. Identification of DNA cleavage- and
560 recombination-specific hnRNP cofactors for activation-induced cytidine deaminase.
561 *Proceedings of the National Academy of Sciences* 2015; **112**: 5791–5796.
- 562 42 Mondal S, Begum NA, Hu W, Honjo T. Functional requirements of AID's higher order
563 structures and their interaction with RNA-binding proteins. *Proceedings of the National*
564 *Academy of Sciences* 2016; **113**: E1545–E1554.
- 565 43 Rouaud P, Vincent-Fabert C, Saintamand A, Fiancette R, Marquet M, Robert I *et al.* The
566 IgH 3' regulatory region controls somatic hypermutation in germinal center B cells. *The*
567 *Journal of Experimental Medicine* 2013; **210**: 1501–1507.

568

569

570 **FIGURE LEGENDS**

571 **Figure 1. Deletion of I γ 1 exon dss decreased RNA pol II pausing and chromatin**
572 **accessibility in the S γ 1 region**

573 (A) Wild type (WT) γ 1 locus and *s-hMT* and *hMT* murine models. Black and grey elements
574 represent gene segments of the γ 1 WT locus. The white elements are gene segments specific to
575 *s-hMT* and *hMT* models and are not present in WT animals. The red fragment corresponds to
576 the sequence containing the I exon donor splice site (dss), retained in the *s-hMT* model and
577 absent in the *hMT* model. P, promoter; I γ 1, γ 1 I exon; I_{hMT}, hMT I exon; S γ 1, γ 1 switch region;
578 CH1, γ 1 constant exon 1. (B) Splenic B cells were isolated from WT, homozygous *s-hMT* and
579 homozygous *hMT* mice and stimulated with LPS + IL4 or LPS. After 2 days stimulation, γ 1
580 GLTs expression relative to GAPDH mRNA expression was monitored by quantitative RT-
581 PCR using S γ 1U primers described in schema A. Expression of γ 1 GLTs in B cells isolated
582 from WT mice and stimulated by LPS + IL4 was normalized to 1. (C-I) Splenic B cells were
583 isolated from homozygous *s-hMT* and *hMT* mice and stimulated with LPS. After 2 days
584 stimulation, the cells were analysed for RNA pol II (C), Ser5P RNA pol II (D) and Ser2P RNA
585 pol II (E) levels in the γ 1 locus by ChIP coupled to quantitative PCR. Ser5P RNA pol II / Ser2P
586 RNA pol II ratios are indicated (F). Cells were also analysed for H3ac (G), H3K9ac (H) and
587 H3K4me3 (I) levels in the γ 1 locus by ChIP coupled to quantitative PCR. Background signals
588 from mock samples with irrelevant antibody were subtracted. Values were normalized to total
589 input DNA. Relative variations of H3K9ac and H3K4me3 marks were expressed after
590 normalization to the value obtained for the promoter. Position and sequence of primers used for
591 quantitative PCR is described in schema A (triangles) and Supplementary table 1. (B-I) Data
592 are means \pm SEM of at least two independent experiments, n=3 to 5 for each genotype. Unpaired
593 two-tailed Student's t test was used to determine significance. ns: non significant; *, P < 0.05,
594 **, P < 0.01, *** P < 0.001, **** P < 0.0001.

595

596 **Figure 2. Treatment with I γ 1 exon dss ASO inhibited γ 1 GLTs constitutive splicing and**
597 **IgG1 class switching in B cells**

598 (A) Antisense oligonucleotide targeting the donor splice site of I γ 1 exon (I γ 1 dss ASO) was
599 designed and synthesized as “vivo-morpholino ASO” permitting passive administration of ASO
600 in cells (Gene Tools, LLC). Targeted γ 1 GLT (uppercase: exon sequence; lowercase: intron
601 sequence) and I γ 1 dss ASO sequences are indicated. I γ 1, γ 1 I exon; S γ 1, γ 1 switch region;
602 CH1 γ 1, γ 1 constant exon 1; dss, donor splice site. (B-G) Splenic B cells were isolated from
603 C57BL/6 mice, stimulated with LPS + IL4 and treated with 2 μ M I γ 1 dss ASO (ASO) or an
604 irrelevant ASO (control) during 2 days (B-C) or 3 days (D-G). (B) Unspliced γ 1 GLTs
605 expression relative to GAPDH mRNA expression was monitored by quantitative RT-PCR using
606 I γ 1-for-Q and S γ 1U-rev-Q primers described in schema A. Expression of γ 1 GLTs in control
607 B cells was normalized to 1. (C-up) RT-PCR was performed using I γ 1-for and C γ 1-rev primers
608 (position described in schema C-middle) to identify constitutively and alternatively spliced
609 transcripts. PCR products were analysed on agarose gels. Expression of actin mRNA is also
610 shown. Molecular markers in base pairs are indicated. Schematic representation of the different
611 γ 1 spliced transcripts is indicated on the right and transcript sequences are given in
612 Supplementary figure 3. One experiment out of three is shown. Quantification of amplification
613 products was done using an Agilent Bioanalyzer. Data are expressed as percentage of each
614 isoforms among the detected transcripts. ND: not detected. (C-middle) Schematic
615 representation of γ 1 spliced transcripts detected in B cells from C57BL/6 mice after treatment
616 with an irrelevant ASO (control) or I γ 1 dss ASO (ASO). Grey hatched lines represent splicing
617 events involving constitutive and alternative splice sites. Donor and acceptor splice sites are
618 indicated in red and green respectively. (C-down) Consensus value (ranging from 0 to 100) of
619 each predicted splice site determined using HSF 3.1 tool. (D) Flow cytometry analysis of

620 purified B cell populations using the indicated cell surface markers. Plots are gated on live cells.
621 The percentage of B220⁺IgG1⁺ cells is indicated. One experiment out of five is shown. (E)
622 Percentage of IgG1 positive cells determined by flow cytometry. (F) Quantification of IgG1 in
623 culture supernatants by ELISA. (G) Post-switch I μ -C γ 1 mRNA expression relative to GAPDH
624 expression was monitored by quantitative RT-PCR. Expression of post-switch mRNAs in
625 control B cells was normalized to 1. Sequence of primers used for RT-PCR and quantitative
626 RT-PCR are indicated in Supplementary table 1. (B and E-G) Data are means \pm SEM of two
627 independent experiments, n=5 to 8 for each group. Unpaired two-tailed Student's t test was
628 used to determine significance. *** P <0.001, **** P <0.0001.

629

630 **Figure 3. Specific IgG1 class switching inhibition in B cells treated by I γ 1 exon dss ASO**

631 Splenic B cells were isolated from *C57BL/6* mice, stimulated with anti-CD40 + IL4 and treated
632 with 2 μ M I γ 1 dss ASO (ASO) or an irrelevant ASO (control) during 2 days (B, E) or 4 days
633 (C, D, F, G). (A) Schematic representation of unspliced ϵ GLT. I ϵ , ϵ I exon; S ϵ , ϵ switch region;
634 CH1 ϵ , ϵ constant exon 1; dss, donor splice site. (B, E) Unspliced γ 1 (B) and ϵ (E) GLTs
635 expression monitored as described in figure 2. I ϵ -for-Q and S ϵ U-rev-Q primers, described in
636 schema A, were used for ϵ GLTs expression determination. (C, F) Post-switch I μ -C γ 1 and I μ -
637 C ϵ mRNA expression monitored as described in figure 2. (D, G) Quantification of IgG1 and
638 IgE in culture supernatants by ELISA. (B-G) Data are means \pm SEM of two independent
639 experiments, n=3 to 4 for each group. Unpaired two-tailed Student's t test was used to determine
640 significance. ns: non significant, ** P < 0.01, *** P <0.001.

641

642 **Figure 4. Defective IgG1 class switching in B cells treated by I μ exon dss ASO**

643 (A) Antisense oligonucleotide targeting the donor splice site of I μ exon (I μ dss ASO) was
644 designed and synthesized as “vivo-morpholino ASO” permitting passive administration of ASO

645 in the cells (Gene Tools, LLC). Targeted μ GLT (uppercase: exon sequence; lowercase: intron
646 sequence) and I μ dss ASO sequences are indicated. I μ , μ I exon; S μ , μ switch region; CH1 μ , μ
647 constant exon 1; dss, donor splice site. (B-E) Splenic B cells were isolated from *C57BL/6* mice,
648 stimulated with LPS + IL4 and treated with 2 μ M I μ dss ASO or an irrelevant control ASO for
649 2 days (B, E) or 3 days (C, D). (B) Constitutively and alternatively spliced μ transcripts analysed
650 as described in figure 2 using I μ -for and C μ -rev primers, described in schema A. (C)
651 Quantification of IgG1 in culture supernatants by ELISA. (D) Percentage of IgG1 positive cells
652 determined by flow cytometry as described in figure 2. (E) Unspliced γ 1 GLTs expression
653 monitored as described in figure 2. (C-E) Data are means \pm SEM, n=3 for each group. Unpaired
654 two-tailed Student's t test was used to determine significance. ns: non significant, * P < 0.05,
655 ** P < 0.01.

656

657 **Supplementary figure 1. Defect of IgG1 class switching in mice lacking I γ 1 dss**

658 (A) Quantification of Ig isotypes (IgM, IgG2b, and IgG1) in sera of homozygous *s-hMT* and
659 *hMT* mice by ELISA. (B-D) Splenic B cells were isolated from homozygous *s-hMT* and *hMT*
660 mice and stimulated with LPS. After 4 days stimulation, amounts of Ig isotypes (IgM, IgG2b,
661 and IgG1) were determined in culture supernatants by ELISA (B). After 3 days stimulation,
662 post-switch I μ -C γ 1 (C) and AID (D) mRNA expression relative to GAPDH mRNA expression
663 was monitored by quantitative RT-PCR. Expression of I μ -C γ 1 or AID in B cells from *s-hMT*
664 mice was normalized to 1. Data are means \pm SEM, n=3 to 4 for each genotype. Unpaired two-
665 tailed Student's t test was used to determine significance. ND: not detected, ns: non significant,
666 **** P < 0.0001.

667

668 **Supplementary figure 2. Similar RNA pol II binding in S μ and S γ 2b regions of *s-hMT* and** 669 ***hMT* mice**

670 Splenic B cells were isolated from homozygous *s-hMT* and *hMT* mice and stimulated with LPS.
671 After 2 days, the cells were analysed for Ser2P RNA pol II (A, B) and Ser5P RNA pol II (C,
672 D) levels in S μ (A, C) and S γ 2b (B, D) regions by ChIP coupled to quantitative PCR.
673 Background signals from mock samples with irrelevant antibody were subtracted. Values were
674 normalized to total input DNA. Primers (triangles) used for quantitative PCR are described on
675 the illustrative schema (bottom). Data are means \pm SEM of at least two independent
676 experiments, n=4 for each genotype. Unpaired two tailed Student's t test was used to determine
677 significance. ns: non significant.

678

679 **Supplementary figure 3. Sequences of γ 1 constitutive and alternative spliced transcripts**

680 The sequences of I γ 1 exon (bold) and CH1 γ 1 exon are indicated. Donor (red) and acceptor
681 (green) splice sites are also represented.

682

683 **Supplementary table 1. Primers used for ChIP, RT-PCR and quantitative RT-PCR**
684 **experiments**

685

686

687

688

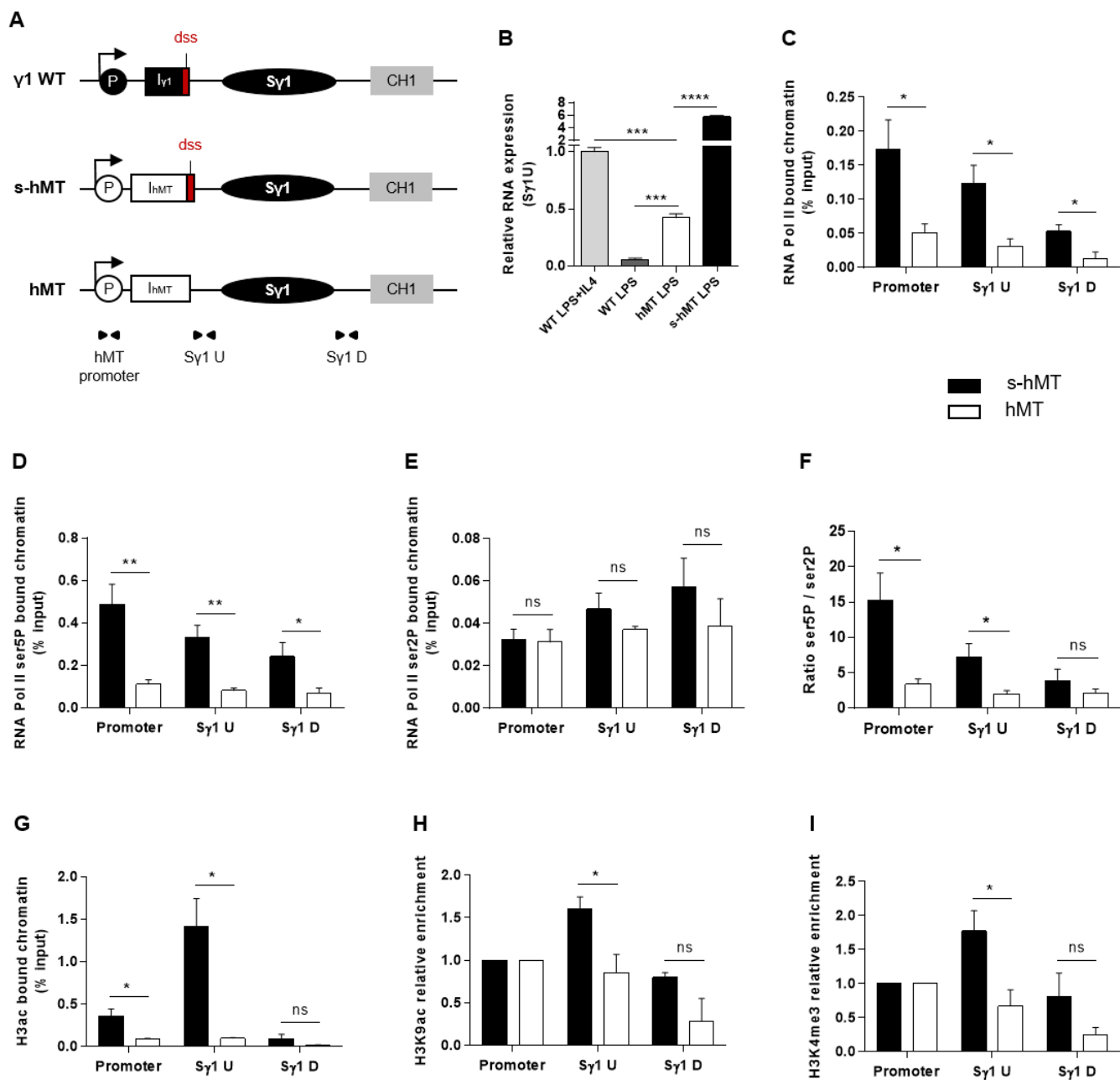


Figure 1

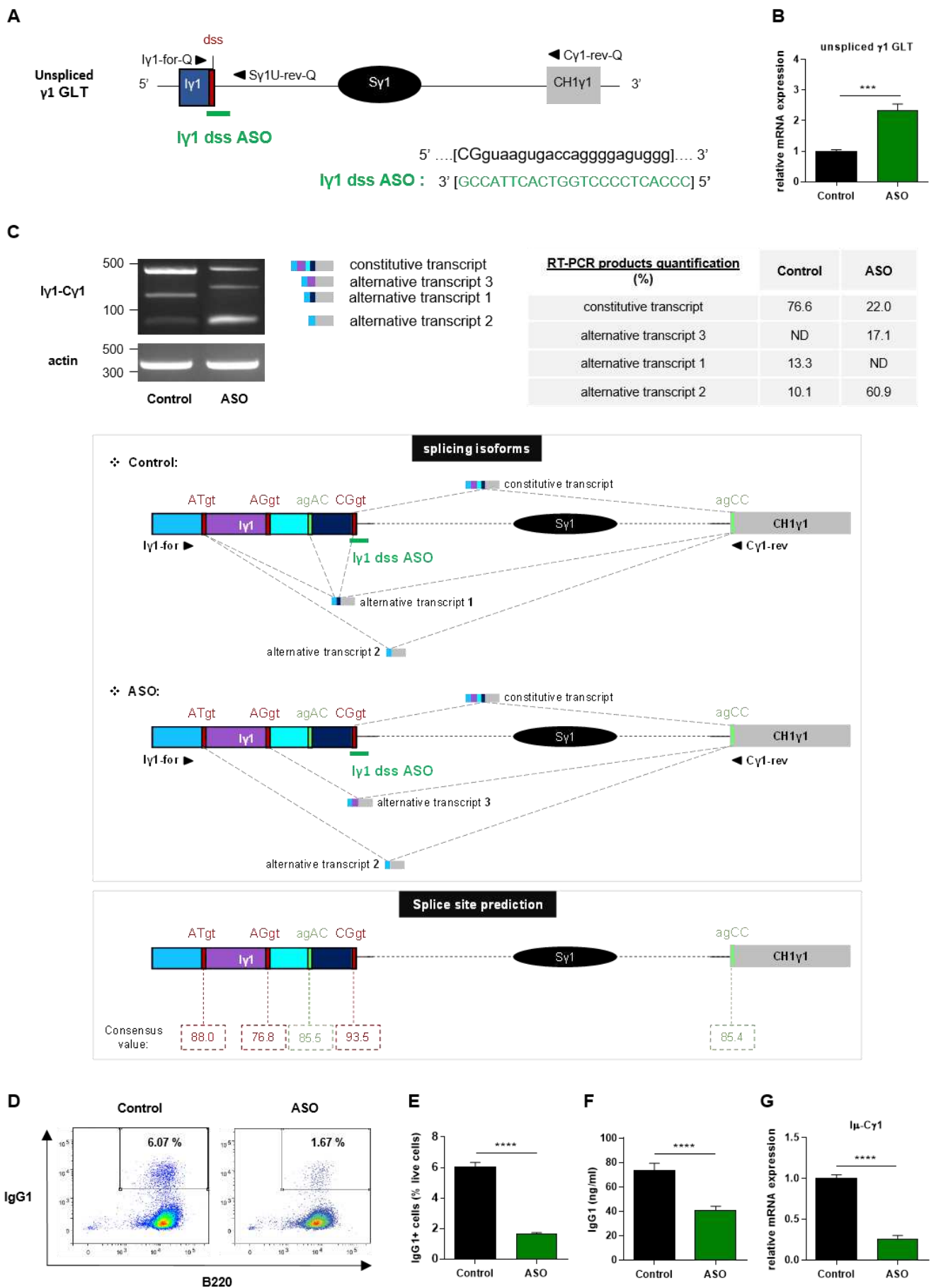


Figure 2

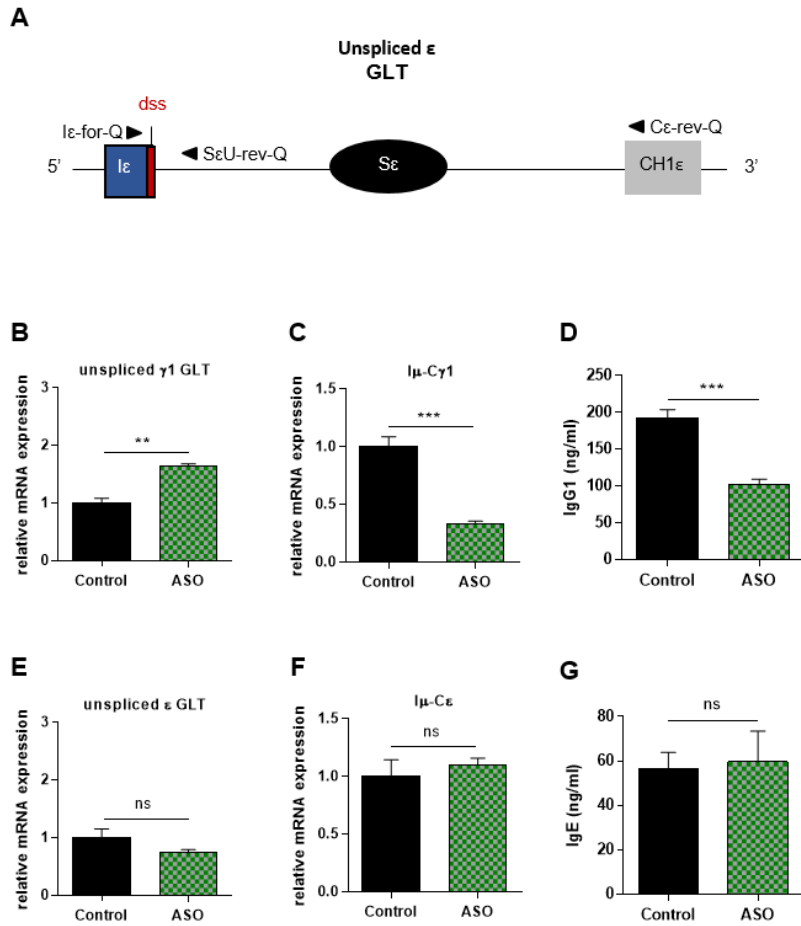


Figure 3

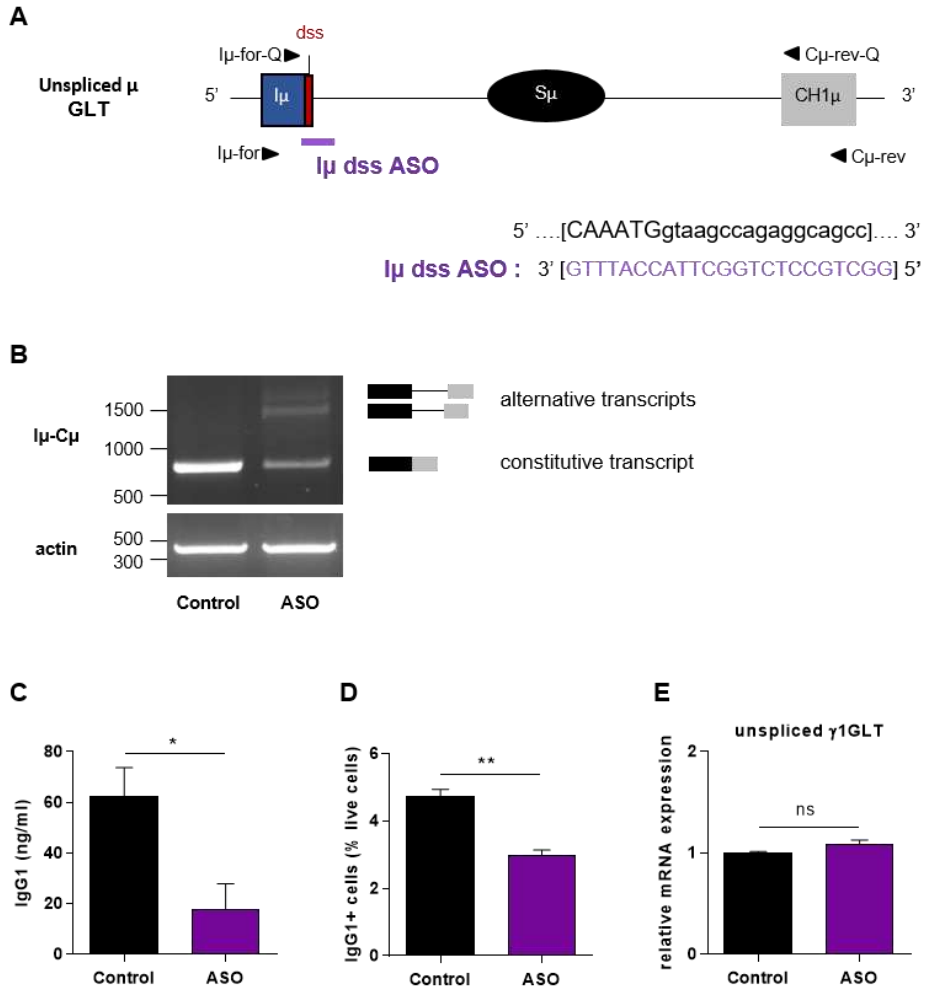


Figure 4